Hindawi
Advances in Civil Engineering
Volume 2021, Article ID 9963450, 11 pages
https://doi.org/10.1155/2021/9963450

Research Article

The Stability Factors' Sensitivity Analysis of Key Rock B and Its Engineering Application of Gob-Side Entry Driving in Fully-Mechanized Caving Faces

Hong-Sheng Wang,[1] **Hai-Qing Shuang**,[2] **Lei Li**,[1] **and Shuang-Shuang Xiao**[1]

[1]*School of Energy Engineering, Xi'an University of Science and Technology, Xi'an, Shaanxi 71005, China*
[2]*School of Safety Science and Engineering, Xi'an University of Science and Technology, Xi'an, Shaanxi 710054, China*

Correspondence should be addressed to Hong-Sheng Wang; cumtwhs@xust.edu.cn

Received 29 March 2021; Accepted 4 May 2021; Published 25 May 2021

Academic Editor: Zizheng Zhang

To reveal the critical factors of the main roof influencing stability of surrounding rocks of roadways driven along goaf in fully-mechanized top-coal caving faces, this paper builds a structural mechanics model for the surrounding rocks based on geological conditions of the 8105 fully-mechanized caving face of Yanjiahe Coal Mine, and the stress and equilibrium conditions of the key rock block B are analyzed, and focus is on analyzing rules of the key rock block B influencing stability of roadways driven along goaf. Then, the orthogonal experiment and the range method are used to confirm the sensitivity influencing factors in numerical simulation, which are the basic main roof height and the fracture location, the length of the key rock block B, and the main roof hardness in turn. It is revealed that the basic main roof height and its fracture location have a greater influence on stability of god-side entry driving. On the one hand, the coal wall and the roof of roadways driven along goaf are damaged, and the deformation of surrounding rocks of roadways and the vertical stress of narrow coal pillars tend to stabilize along with the increase of the basic main roof height. On the other hand, when the gob-side entry is located below the fracture line of the main roof, the damage caused by gob-side entry is the most serious. Therefore, on-site gob-side entry driving should avoid being below the fracture line of the main roof. At last, industrial tests are successfully conducted in the fully-mechanized top-coal caving faces, 8105 and 8215, of Yanjiahe Coal Mine.

1. Introduction

Adoption of the narrow coal pillar gob-side entry driving technique can efficiently increase recycling efficiency of coal resources and control effect of surrounding rocks of roadways. The technique has been widely used in China, but stability of surrounding rocks of roadways driven along goaf has limited further development of the technique [1–17]. Research has shown that there are multiple factors that influence the stability. References [1–17] are the Chinese scholars' findings. Among them, Bai et al. [1, 2] built an arc-shaped triangular block structural mechanism model for surrounding rocks based on stress conditions of the working face; Li [3, 4] analyzed influence of big and small structures of roadways driven along goaf in fully-mechanized top-coal caving face on stability of surrounding rocks; Zhang et al. [5, 6] analyzed deformation features of surrounding rocks of gob-side entry retaining in the fully-mechanized coal face with top-coal caving and influence of multiple factors on deformation and stress of gob-side entry retaining with entry-in packing in the top-coal mining face; Wang et al. [7, 8] discussed influence of three different fracture locations of the overlaying main roof of roadways driven along goaf on stability of surrounding rocks of the roadway and rational width of the narrow coal pillar based on the fracture line location of key rock B in the main roof; Zhu et al. [9] studied the main factors affecting the deformation of the filling body; Xie [10] adopted UDEC simulation to analyze rules of six factors, such as support technique and influencing stability of surrounding rocks of gob-side entry retaining in top-coal

mining faces; Zhang et al. [11, 12] analyzed four different Chinese coal mining sites and evaluated the influencing factors; Meng and Li [13] studied parameters' sensitivity of bolt support in gob-side entry driving and found that the main influence parameters were bolt pretightening force and bolt interval; Yuan et al. [14] studied the dynamic effect and control mechanism of key strata in the immediate roof; Bai et al. [15] studied the stress state and the deformation failure mechanism of the heading adjacent to the advancing working face roof structure; Li et al. [16] studied the in situ stress distribution characteristics of the rock mass near different slope angles' hillslope surfaces; Wang et al. [17] studied the stability of the concrete artificial side introduced to stabilize a gob-side entry.

The above analysis suggested that stability of the key rock block B could directly influence stability of the large structure of roadways driven along goaf and indirectly influence the stress environment of the small structure. The former mainly adopted theoretical analysis and quantitative experiments to analyze stability of the large structure of roadways driven along goaf, while the latter mainly analyzed influence of factors, such as support parameters, on stability of surrounding rocks of roadways based on numerical simulation. Few of them analyzed sensitivity of major factors of the main roof on stability of surrounding rocks of roadways driven along goaf in fully-mechanized top-coal caving faces. In view of the research gap, this paper built a structural mechanics structure for surrounding rocks of the key rock block B to quantitatively analyze influence of main roof factors on stability of surrounding rocks. Based on mining technical conditions of Yanjia Coal Mine in Binchang Mining Area, four factors of the main roof are confirmed. Combining the orthogonal experimental scheme, the author analyzes sensitivity of the four main roof factors and conducts a univariate analysis of the two factors with a stronger sensitivity. Research findings are successfully applied to the 8105 working face and further promoted in the 8215 working face. Therefore, research results of this paper can contribute to popularization of gob-side entry driving technique under similar geological conditions.

2. Mechanical Analysis of the Key Rock Block B in the Main Roof

2.1. Building of the Key Rock Block B Mechanical Model. Currently, the narrow coal pillar gob-side entry driving technique is prevailing in China. After the overlaying rock of the goaf in the working face of the former sector stabilizes, the roadway driven along goaf starts. Figure 1 shows the structure of the fracture line of the main roof surrounding rock structure within the coal wall during gob-side entry in a fully-mechanized top-coal caving face.

Below is the stress analysis of the key rock block B [18]: the resultant force of shear force and horizontal thrust of the key rock block A on the key rock block B is R_{AB} and T_{AB}, respectively; the resultant force of vertical shear force and horizontal thrust of the key rock block C on the key rock block B is R_{BC} and T_{BC}, respectively; the dead load of the soft stratum above the block B is F_R; the dead load resultant force of the block B is F_Z; the support force of the goaf waste rock for the block B is F_G; the support force of the damaged immediate roof in the section without top-coal caving for the block B is F_D; the support force of the immediate roof in the narrow coal pillar for the block B is F_S; the support force of the immediate roof of the physical coal wall for the block B is F_M; the rotation angle of the block B is θ. The stress situations of block B are shown in Figure 2. To put the surrounding rock structure of the block B in an equilibrium state, the block B should achieve equilibrium of stress horizontally and vertically after its stability. Besides, there is no allowance for slipping and rotation.

(1) Vertical:

$$\begin{aligned} \sum F_y &= 0, \\ R_{AB} + F_M + F_D + F_G - 2R_{BC} - F_R - F_Z &= 0. \end{aligned} \tag{1}$$

(2) Horizontal:

$$\begin{aligned} \sum F_x &= 0, \\ T_{AB} - 2T_{BC}\cos\alpha &= 0, \end{aligned} \tag{2}$$

where α stands for the base angle of the key rock block B (°).

(3) Conditions for the key rock blocks B and A to lose stability are as follows [19]:

$$\begin{aligned} T_{AB}\tan\varphi &\geq R_{AB}, \\ \frac{T_{AB}}{L_1 a} &\leq \eta\sigma_c, \end{aligned} \tag{3}$$

where $\tan\varphi$ stands for the friction factor between the two rock blocks, $(T_{AB}/L_1 a)$ stands for the average crushing stress between the two rock blocks, MPa, η stands for the special coefficient of the stress analysis between the two rock blocks, and σ_C stands for the compressive strength of the rock block B, MPa.

2.2. Analysis of Factors Influencing Stability of the Key Rock Block B. Based on structural stress analysis of the key rock block B, it can be seen that the length of the block B can directly influence the area of the immediate roof that it covers after rotary subsidence. Since the dead load of the soft stratum is above the key rock block B, F_R, the dead load of the key rock block B, F_Z, will cause different degrees of contact with the immediate rock or the goaf waste rocks; the value of F_G, F_D, F_S, and F_M is thus decided. During the rotary subsidence process, if the block B does not contact the immediate rock and the goaf waste rocks, or it does contact them but generate no compression, the immediate roof or the goaf waste rocks cannot provide support stress for the main roof. When the block B contacts the two and generates compression, the latter will provide support stress for the main roof. The value of the stress is closely related to the compression rate of the immediate roof and the goaf waste

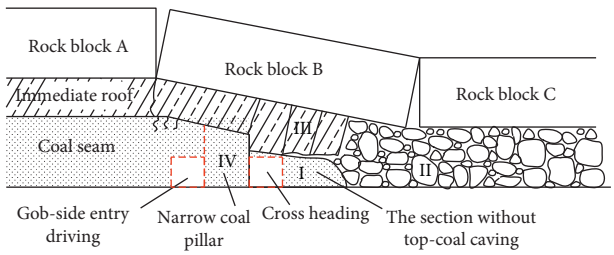

Figure 1: Surrounding rock structural mechanics model during gob-side entry in a fully-mechanized top-coal caving face.

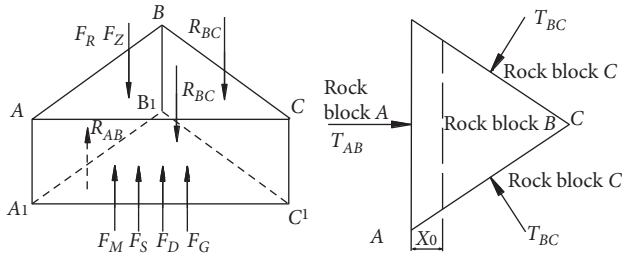

Figure 2: Structural stress of surrounding rocks of the key rock block B.

rocks, and the compression rate has a close bearing on thickness, strength, and swell factor of the immediate roof and the coal strata and the mechanical strength of goaf waste rocks.

When the fracture line location of the main roof is different [8], the horizontal stress remains the same, but the vertical stress of the key rock block B changes. See the following:

(1) When the fracture line of the main roof is within the physical coal wall,

Under the condition, the vertical stress changes as follows:

$$R_{AB} + F_M + F_D + F_G + F_S - 2R_{BC} - F_R - F_Z = 0. \quad (4)$$

(2) When the fracture line of the main roof is outside the narrow coal pillar,

Under the condition, there is no F_M on the block B vertically, and the stress changes as follows:

$$R_{AB} + F_D + F_G - 2R_{BC} - F_R - F_Z = 0. \quad (5)$$

(3) When the fracture line of the main roof is just above the roadway,

Under the condition, there is no F_M and F_S on the block B vertically, and the stress changes as follows:

$$R_{AB} + F_D + F_G + F_S - 2R_{BC} - F_R - F_Z = 0. \quad (6)$$

To sum up, different fracture line locations of the main roof will directly influence the value of the vertical stress on the block B. Besides, during the rotary subsidence process, different compression ratios with the immediate roof can result in different value of support stress. Therefore, there are many factors influencing stability of the block B. It is hard to accurately and quantitatively describe its value theoretically and in practices. It is necessary to turn to the numerical simulation to analyze influence of factors of the basic roof on stability of surrounding rocks in gob-side entry in fully-mechanized top-coal caving faces.

3. Confirmation of Sensitivity of Major Factors of the Main Roof

3.1. Confirmation of Influencing Factors. The working face of Yanjiahe Coal Mine features a single-wing main roadway belt layout. In order to efficiently connect working faces and efficiently control deformation of the surrounding rock of roadways, the narrow coal pillar gob-side entry is adopted, and favorable technical and economic efficacy is achieved [20–23], but geological conditions of Yanjiahe Coal Mine are complex, and the working face mine pressure behaviors and drill peeping analysis show that storage condition changes of the main roof are huge [2, 3]. Based on geological conditions of Yanjiahe Coal Mine, rules of four factors, including the main roof height and strength, the length of the key rock block B, and the fracture location of the main roof, in influencing stability of surrounding rocks of roadways driven along goaf is analyzed.

3.2. Orthogonal Experiment. The orthogonal experimental scheme is adopted to analyze different degrees of influence of four factors of the main roof on stability of surrounding rocks of roadways driven along goaf. The experimental scheme and the four factors are shown in Tables 1 and 2. Under the same bolt support, the deformation of surrounding rocks of roadways is an index to measure influence of different factors on stability of surrounding rocks of roadways. According to the orthogonal experimental scheme, the sensitivity of the four factors is ranked in order, and the two of them with a greater sensitivity are selected for the univariate analysis as to their influence on stability of surrounding rocks of roadways.

3.3. Modeling. Based on geological conditions of the 8105 fully-mechanized top-coal caving face, the authors adopt UDEC2D4.0 to build the numeric calculation model [21, 24, 25]. The constitutive relation between the rock block and the surrounding rocks features a Mohr–Coulomb model. The physical mechanical parameters of the rock mass are shown in Table 3. The belt cross-heading fracture surface of 8105 is 4000 mm × 3000 mm; and, the combined support featuring high-intensity deformed steel bar resin bolt + high preload + cable reinforcement + roof bolting with bar and wire [18, 22] is adopted. During the simulation process, the neighboring caving faces are first excavated and balanced; and, then comes the gob-side entry driving. The whole process should lay out corresponding stress and displacement monitoring points.

Table 1: Experimental factors and levels.

Level	Factor			
	Main roof height (m)	Main roof hardness (MPa)	Length of the key rock block B (m)	Fracture position of the main roof (m)
1	0	Soft/25	16	Inside the coal wall 2 m
2	5	Medium-hard/35	18	Right above the roadway
3	10	Hard/45	20	Outside the coal wall 2 m

3.4. Analysis of the Orthogonal Experimental Scheme. The "cross-measurement method" is adopted to measure deformation of surrounding rocks. Then, the range method is used to comparatively analyze the deformation of four factors under three levels. The deformation of surrounding rocks is shown in Table 2.

From Table 2, it can be seen that the range of the four factors influencing overall stability of surrounding rocks of roadways, including the main roof height and hardness, the length of the key rock block B, and the fracture location, based on the orthogonal univariate analysis is 393.54 mm, 29.19 mm, 84.20 mm, and 93.03 mm, respectively; the range of the four factors influencing stability of surrounding rocks on two ribs of roadways is 173.09 mm, 54.59 mm, 3.96 mm, and 29.02 mm, respectively; and, the range of four factors influencing stability of the roof-to-floor surrounding rocks is 220.45 mm, 25.40 mm, 80.24 mm, and 90.18 mm, respectively.

Thus, the degree of influence of the four factors of the main roof on stability of surrounding rocks of roadways driven along goaf can be ranked as follows: the main roof height > the main roof fracture location > the length of the key rock block B > the main roof hardness. The degree of influence of the four factors on surrounding rocks on two ribs of roadways can be ranked as follows: the main roof height > the main roof hardness > the main roof fracture location > the length of the key rock block B. The degree of influence of the four factors on the roof-to-floor surrounding rocks can be ranked as follows: the main roof height > the main roof fracture location > the length of the key rock block B > the main roof hardness. It can be seen that the main roof height and the main roof fracture location are two factors with a greater sensitivity.

4. Sensitivity Univariate Analysis of the Main Roof

4.1. Simulation Scheme. In order to further analyze the influence of the main roof height and its fracture location on stability of roadways driven along goaf, the univariate analysis is adopted. The simulation scheme is shown in Table 4. The main roof hardness is set to be medium-hard, and the length of the key rock block B is set to be 18 m.

4.2. Univariate Analysis Scheme

4.2.1. Influence of the Main Roof Height on Stability of Surrounding Rocks of Roadways. The average value of the deformation of surrounding rocks of roadways and the vertical stress value before and after coal pillar driving of nine schemes included in Table 2 are shown in Figure 3.

From Figure 3, it can be seen that the coal pillar stress before driving is larger than that after driving. Before the roadway driving, the overlaying strata of neighboring caving faces is basically stable, the key rock block B is in an equilibrium state, and the stress on the coal wall is concentrated. In Schemes 1–3, Schemes 4–6, and Schemes 7–9, the vertical stress scope in the central position of the narrow coal pillar is 7.41~9.43 MPa. This suggests that the influence of the main roof height and the fracture location on the coal pillar stress before the roadway driving is not significant. After the roadway driving, the stress of surrounding rocks of roadways needs to be redistributed, and the stress peak value transfers to the inside of the coal. At the moment, the coal pillar is in the stress declining area. In Schemes 1–3, Schemes 4–6, and Schemes 7–9, the average vertical stress of the coal pillar is within the range of 4.36~5.03 MPa, 1.56~2.67 MPa, and 2.07~2.38 MPa, respectively. This suggests that, when the main roof height is 0 m, the narrow coal pillar has a greater support stress, F_S, for the key rock block B. Along with the increase of the main roof height, the support stress of the main roof in the section without coal and the goaf waste rocks for the key rock block B is F_D and F_G, respectively, thus reducing the compression of the key rock block B on the immediate roof above the coal pillar.

From Figure 3, it can be seen that the relative deformation on the two ribs of the roadway in Schemes 1–9 is 151.50%, 141.45%, 136.04%, 163.12%, 143.72%, 131.24%, 168.07%, 76.96%, and 146.21% of the roof-to-floor relative deformation. Thus, it can be judged that deformation on two ribs dominates in roadways driven along goaf in fully-mechanized top-coal caving faces. The relative deformation on two ribs in Schemes 1–3, Schemes 4–6, and Schemes 7–9 is 274.95~322.25 mm, 315.01~368.86 mm, and 295.57 mm~390.31 mm, respectively; the deformation is small in Schemes 1–3. The deformation in Schemes 4–6 and Schemes 7–9 is almost the same. After roadways driven along goaf, the surrounding rocks of roadways obtain timely support. The surrounding rocks' stress is quickly redistributed. Relying on bolt and cable support, surrounding rocks of roadways form a small structure. With the rotary subsidence of the key rock block B, the support stress provided by the immediate roof and the physical coal wall right above the narrow coal pillar, F_S and F_M, increases and the stress of the narrow coal pillar and the physical coal wall concentrates, thus resulting in expansion and deformation of surrounding rocks.

4.2.2. Influence of the Main Roof Fracture Location on Stability of Surrounding Rocks of Roadways. The deformation of surrounding rocks of roadways in Schemes 1~3,

Table 2: Orthogonal experimental scheme and simulation results.

Serial number	Factors				Total deformation of surrounding rocks (mm)	Rib-to-rib relative deformation (mm)	Roof-to-floor relative deformation (mm)
	Main roof height	Main roof hardness	Length of the key rock block B	Fracture location			
1	1	1	3	2	479.7	288.97	190.73
2	2	1	1	1	880.29	515.70	364.59
3	3	1	2	3	775.7	447.07	328.63
4	1	2	2	1	455.28	282.25	173.03
5	2	2	3	3	755.02	445.23	309.79
6	3	2	1	2	849.82	482.32	367.50
7	1	3	1	3	413.1	259.00	154.10
8	2	3	2	2	893.39	388.55	504.84
9	3	3	3	1	741.64	440.42	301.22
Average value 1	449.36	711.90	658.79	740.97	Total deformation of surrounding rocks		
Average value 2	842.90	686.71	742.99	692.40			
Average value 3	789.05	682.71	679.54	647.94			
Range	**393.54**	**29.19**	84.20	93.03			
Average value 1	276.74	417.25	391.54	386.61	Rib-to-rib relative deformation		
Average value 2	449.83	403.27	395.50	412.79			
Average value 3	456.60	362.66	396.13	383.77			
Range	**173.09**	54.59	**3.96**	29.02			
Average value 1	172.62	294.65	267.25	354.36	Roof-to-floor relative deformation		
Average value 2	393.07	283.44	347.49	279.61			
Average value 3	332.45	320.05	283.41	264.17			
Range	**220.45**	**25.40**	80.24	90.18			

Table 3: Physical mechanical parameters of the rock mass.

Lithology	Bulk modulus (GPa)	Shear modulus (GPa)	Internal friction angle (°)	Cohesion (MPa)	Thickness (m)
Coarse-grained sandstone	11	9	36	4.0	7
Sandy mudstone	16	12	32	3.5	20
Siltstone	20	16	33	6.0	10
Siltstone	20	16	33	6.0	6
No. 5^{-1} coal seam	8	6	28	1.5	3
Mudstone	6	5	28	4.0	2
Sandy mudstone	16	12	32	3.5	2
No. 5^{-2} coal seam	8	6	28	1.5	2
Mudstone	6	5	28	4.0	3
Sandy mudstone	16	12	32	3.5	3
Siltstone	20	16	33	6.0	3
Sandy mudstone	16	12	32	3.5	8
Siltstone	20	16	33	6.0	4
No. 7 coal seam	8	6	28	1.5	2
Mudstone	6	5	28	4.0	2
Sandy mudstone	16	12	32	3.5	1.5
No. 8 coal seam	8	6	28	1.5	7
Sandstone	12	10	38	7.0	28.5

Table 4: Simulation scheme.

Main roof height (m)	Main roof fracture location		
	Inside the coal wall 2 m	Outside the narrow coal pillar 2 m	Right above the roadway
0	Scheme 1	Scheme 2	Scheme 3
5	Scheme 4	Scheme 5	Scheme 6
10	Scheme 7	Scheme 8	Scheme 9

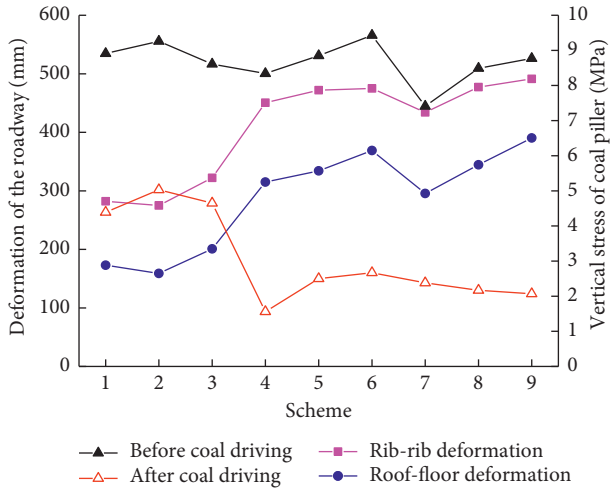

Figure 3: Display of relative deformation of surrounding rocks of roadways and vertical stress of the coal pillar.

Schemes 4~6, and Schemes 7~9 is shown in Figures 4(a)–4(c), respectively.

From Figure 4, it can be seen that deformation of surrounding rocks of roadways driven along goaf mainly happens in the physical coal wall and the roof side. Under the same height but different basic roof fracture locations, the deformation of surrounding rocks of roadways is different. Below is a detailed analysis.

When the main roof height is 0 m, the deformation of the coal wall side, the roof side, the coal pillar side, and the floor side in roadways shown in Schemes 1–3 is 241.40 mm, 117.29 mm, 40.85 mm, 55.73 mm, 210.84 mm, 109.53 mm, 64.11 mm, 49.40 mm, 214 mm, 152.12 mm, 108.25 mm, and 48.76 mm, respectively.

At the moment, there is no immediate roof above the coal strata, thus resulting in no goaf waste rock support force, F_G, for the key rock block B. When the basic main roof fracture location is right above roadways, the key rock block B will rotate and sink directly on the roof side of the roadway and the side of the narrow coal pillar. Under the condition, the deformation of surrounding rocks of roadways is larger than that under the other two conditions.

When the main roof height is 5 m, the deformation of the physical coal wall side, the roof side, the coal pillar side, and the floor side is 360.9 mm, 229.73 mm, 89.68 mm, 85.23 mm, 386.14 mm, 248.3 mm, 85.87 mm, 85.87 mm, 343.56 mm, 277.26 mm, 131.39 mm, and 91.6 mm, respectively.

When the main roof height is 10 m, the deformation of the physical coal wall side, the roof side, the coal pillar side, and the floor side is 338.99 mm, 219.34 mm, 95.11 mm, 76.24 mm, 365.29 mm, 263.28 mm, 111.97 mm, 81.28 mm, 364.9 mm, 318.25 mm, 126.38 mm, and 72.06 mm, respectively. At the moment, there is an immediate roof between the coal strata and the main roof. After roadway driving and rotary subsidence of the key rock block B, the block B might receive the stress from the main roof, F_D, F_S, F_M, and F_G. Through the immediate roof, it will function on the coal

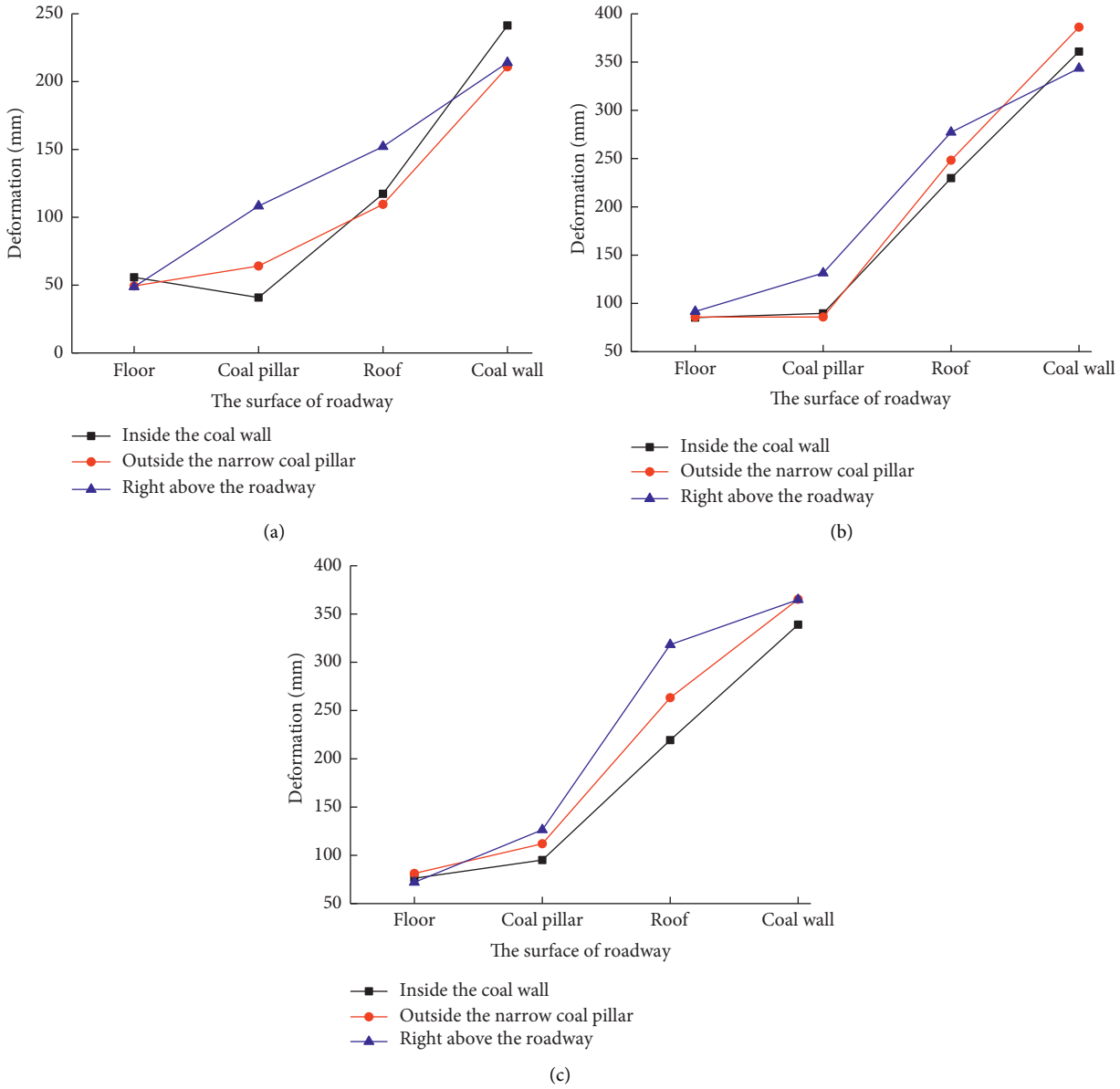

Figure 4: Deformation of surrounding rocks of roadways when the main roof fracture location is different. (a) The main roof height is 0 m. (b) The main roof height is 5 m. (c) The main roof height is 10 m.

pillar, the roadway roof, the physical coal wall, and the goaf to achieve an equilibrium state. When the main roof fracture location is right above roadways, the compression rate between the narrow coal pillar and the immediate roof right above roadways is relatively large, and the stress concentration is high. Consequently, the deformation of surrounding rocks of the narrow coal pillar side and the roof side becomes larger than that under the above two conditions.

Therefore, in order to reduce the stress concentration degree of the narrow coal pillar side and right above roadways, it is necessary to avoid laying gob-side entry driving right below the main roof fracture location. In this way, the bolt or the cable will control deformation of surrounding rocks of roadways more easily.

5. Engineering Application Analysis

Based on the above research, engineering application analysis is conducted on two fully-mechanized top-coal caving faces, namely, 8105 and 8215.

5.1. 8105 Fully-Mechanized Top-Coal Caving Face. 8105 track transport roadway drives along the 8104 goaf. It is necessary to master the main roof fracture line location on the 8105 top-coal caving face. Therefore, the 8103 track transport roadway and the 8105 belt transport roadway lay the probing drills on the 8102 goaf and the 8106 goaf. Measurement shows that the basic main fracture line is located within the physical coal wall, which is 3.42~3.87 m away from the goaf

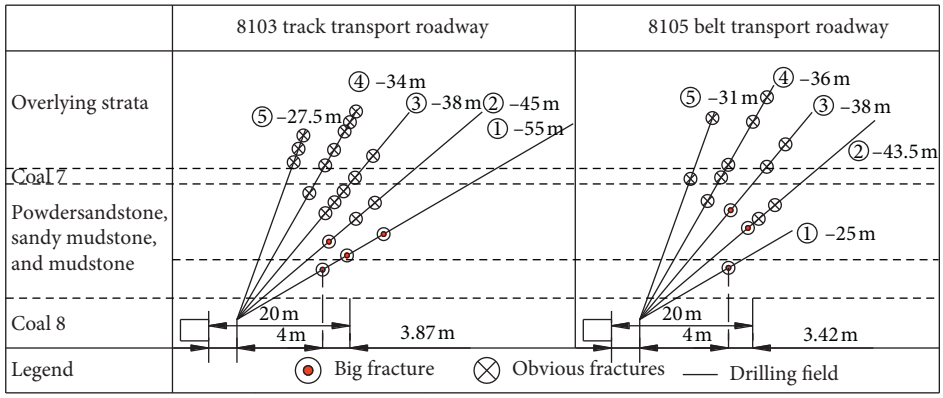

Figure 5: Probing results of the main roof fracture location.

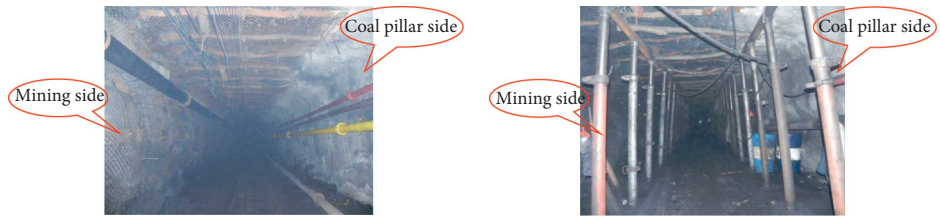

(a) (b)

Figure 6: Control effects of surrounding rocks on the belt cross-heading of the 8105 caving face. (a) One year late after driving. (b) Influenced by mining.

boundary. Therefore, the coal pillar width should not be within the range of 3.42~3.87 m [8, 22]. (See Figure 5) The numerical simulation analysis is adopted to analyze changing rules of surrounding rock deformation and coal pillar and seam floor vertical stress under different coal pillar width. Finally, the reasonable width of the coal pillar is 6.5 m. After 20 days of roadway driving, the surrounding rocks are basically stable, and the maximum roof-to-floor and two-rib displacement is 118 mm and 65 mm, respectively. Influenced by the caving face excavation, the maximum roof-to-floor and two-rib displacement is 200~420 mm and 380~600 mm, respectively. The control effect of surrounding rocks of roadways is shown in Figure 6.

5.2. 8215 Fully-Mechanized Top-Coal Caving Face. The 8215 track transport roadway drives along the 8214 goaf boundary, and the coal pillar width of the coal section is 8.0 m. Six monitoring stations are laid out to monitor surrounding rocks of roadways. After 20 days of roadway driving, the surrounding rocks are basically stable, the bolt and cable working conditions are favorable, and the maximum roof-floor and two-rib displacement amount of six monitoring stations is 100~160 mm and 80~100 mm, respectively. Influenced by excavation, the maximum roof-floor and two-rib displacement amount is 220~460 mm and 340~620 mm, respectively. The stress variation rules of the coal monitored by the monitoring station 2 are shown in Figure 7. 064Y, 065Y, and 066Y in Figure 7 represent the surrounding rock stress 4 m within the narrow coal pillar, 5 m within the physical coal wall, and 10 m within the physical coal wall.

From Figure 7, it can be seen that the stress 4 m within the coal pillar is low and changes within the range of 0.1~0.2 MPa. The stress 5 m within the physical coal wall is large. If not influenced by excavation, it changes within the range of 0.1~0.6 MPa, and if influenced by excavation, it changes within the range of 0.7~0.8 MPa. The stress 10 m within the physical coal wall is relatively large. If not influenced by excavation, the change is within the range of 0.1~0.8 MPa; if influenced by excavation, the peak stress value can reach 10.9 MPa. Results suggest that, if the coal is not influenced by excavation, the surrounding rock stress is relatively small; if influenced by excavation, the surrounding rock stress is transferred to be within the physical coal wall. However, the roadways driven along goaf far always in the stress decline area, which is beneficial to the surrounding rock control of roadways.

Changing rules of the surrounding rock deformation and the coal stress suggest that roadways, influenced by excavation, are efficiently controlled, thus meeting requirements of the working face stopping [20, 23]. In order to master the main roof fracture line of the 8215 caving face, probing drills are laid by the 8215 track transport roadway to the overlaying strata on the 8214 goaf, and the probing results are shown in Figure 8.

From Figure 8, the large fractures concentrate above the coal pillar near the goaf. Their distance away from the coal pillar margin is short, namely, 1.22 m, 3.42 m, and 4.15 m, respectively. Areas with obvious fractures are gradually away from Coal 8, and they are mainly distributed near the upper

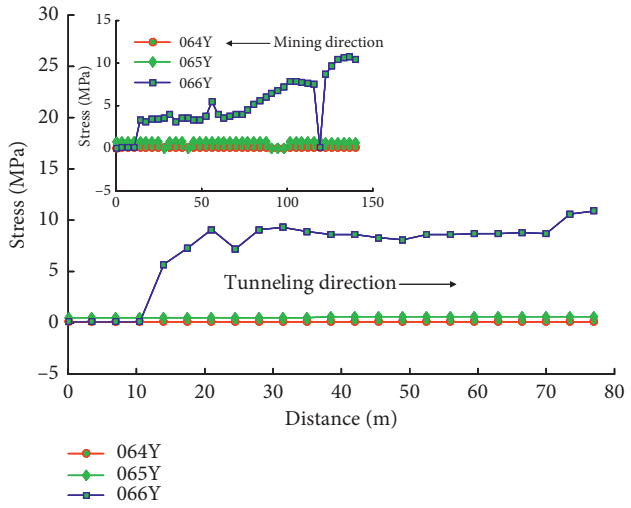

Figure 7: Changing rules of the coal stress.

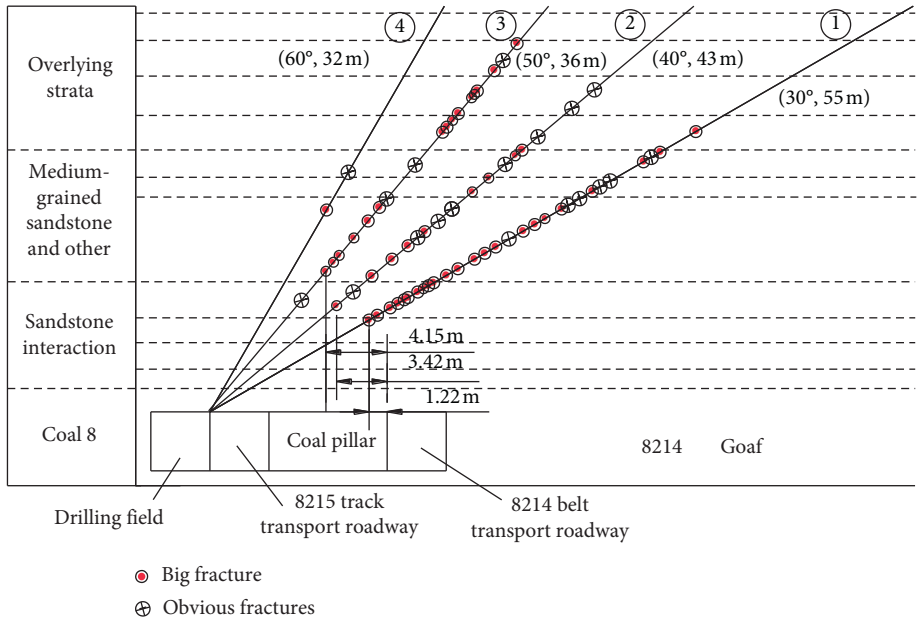

Figure 8: Probing results of the main roof fracture location.

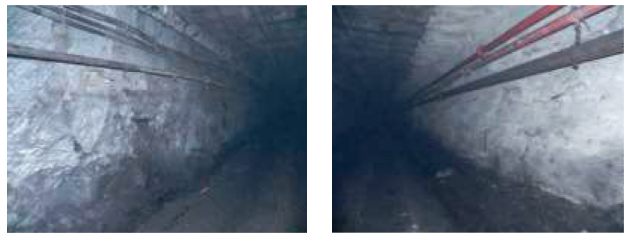

(a) (b)

Figure 9: Surrounding rock control effect of the 8215 rail transportation roadway ten months late after driving. (a) Mining side. (b) Coal pillar side.

right of the coal pillar in goaf and far away from the coal pillar margin. It suggests that it is reasonable to set the coal pillar to be 8.0 m, which can avoid putting the roadway right under the basic fracture line, and the surrounding rock control effects are shown in Figure 9.

6. Conclusions

This paper builds the structural mechanics model of the key rock block B, points out that equilibrium of the key rock block B should meet conditions not to lose equilibrium horizontally and vertically, qualitatively analyzes the influence of the main roof factors on stress of the key rock block B, and places particular emphasis on stress-changing rules of the key rock block B vertically under three different fracture locations of the main roof.

Based on mining technical conditions of Yanjiahe Coal Mine in Binchang Mining Area, four factors of the main roof are confirmed, including the main roof height and hardness, the length of the key rock block B, and the main roof fracture location. The orthogonal experiment is used to set nine plans; the range method is employed to confirm the sensitivity order of the main roof, which is as follows: the main roof height > the main roof fracture location > the length of the key rock block B > the main roof strength.

The univariate method is adopted to analyze the influence of the main roof height and the fracture location on stability of surrounding rocks of roads in fully-mechanized caving faces. It is found that surrounding rock deformation during roadways driven along goaf happens in the physical coal wall and the roof side. The deformation of surrounding rocks of roadways and the vertical stress of the narrow coal pillar tend to stabilize along with the increase of the main roof height. Meanwhile, the roadway driving right below the basic fracture line should be avoided.

The engineering application effects suggest that the narrow coal pillar layout is reasonable on the 8105 and 8215 caving face, which can avoid putting the main roof fracture location right above the roadway. The surrounding rocks of the driving roadways are in a low-stress environment, and the surrounding rocks of the roadways are efficiently controlled. All these have guaranteed safe and efficient stopping of caving faces.

Data Availability

The data used to support the findings of this study are included within the article.

Conflicts of Interest

The authors declare that there are no conflicts of interest regarding the publication of this paper.

Authors' Contributions

Hong-sheng Wang conceived of the research. Hong-sheng Wang and Hai-qing Shuang analyzed the data and wrote the paper. Lei Li and Shuang-shuang Xiao participated in the design of the study and verified the results. All authors have read and approved the final manuscript.

Acknowledgments

This work was supported by the National Natural Science Foundation of China (no. 51974231) and National Basic Research Program of China (973 Program) (no. 2015CB251600).

References

[1] J. B. Bai, W. J. Wang, and C. J. Hou, "Control mechanism and support technique about gateway driven along goaf in fully mechanized top coal caving face," *Journal of China Coal Society*, vol. 25, no. 5, pp. 478–481, 2000.

[2] Z. Zhang, J. Bai, Y. Chen, and S. Yan, "An innovative approach for gob-side entry retaining in highly gassy fully-mechanized longwall top-coal caving," *International Journal of Rock Mechanics & Mining Sciences*, vol. 80, no. 12, pp. 1–11, 2015.

[3] C. J. Hou and X. H. Li, "Stability principle of big and small structures of rock surrounding roadway driven along goaf in fully mechanized top coal caving face," *Journal of China Coal Society*, vol. 26, no. 1, pp. 1–7, 2001.

[4] X. H. Li, "Deformation mechanism of surrounding rocks and key control technology for a roadway driven along goaf in fully mechanized top-coal caving face," *Journal Coal Science Engineering*, vol. 9, no. 1, pp. 28–32, 2003.

[5] D. S. Zhang, X. B. Mao, and W. D. Ma, "Testing study on deformation features of surrounding rocks of gob-side entry retaining in fully-mechanized coal face with top-coal caving," *Chinese Journal of Rock Mechanics and Engineering*, vol. 21, no. 3, pp. 331–334, 2002.

[6] D. S. Zhang, L. Q. Ma, and X. X. Miao, "Factor analysis on deformation of gob-side entry retaining with entry-in packing in top-coal caving mining face," *Journal of China University of Ming Technology*, vol. 35, no. 1–6, pp. 331–334, 2006.

[7] H. S. Wang, *Research on the Creep Character and its Stability Control Technology of Gob-Side Entry's Narrow Side*, China University of Mining and Technology, Xuzhou, China, 2011.

[8] H. S. Wang, D. S. Zhang, S. G. Li, L. Wang, and L. Z. Wang, "Rational width of narrow coal pillar based on the fracture line location of key rock B in main roof," *Journal of Mining and Safety Engineering*, vol. 31, no. 1, pp. 10–16, 2014.

[9] C. Q. Zhu, X. X. Miao, and Z. Liu, "Mechanical analysis on deformation of surrounding rock with road-in packing of gob-side entry retaining in fully-mechanized sub-level caving face," *Journal of Coal Science and Engineering*, vol. 14, no. 1, pp. 24–28, 2008.

[10] W. B. Xie, "Influence factors on stability of surrounding rocks of gob-side entry retaining in top-coal caving mining face," *Chinese Journal of Rock Mechanics and Engineering*, vol. 23, no. 18, pp. 3059–3065, 2004.

[11] N. Zhang, L. Yuan, C. L. Han, J. H. Xue, and J. G. Kan, "Stability and deformation of surrounding rock in pillarless gob-side entry retaining," *Safety Science*, vol. 50, no. 4, pp. 593–599, 2012.

[12] N. Zhang, C. Liu, and P. Yang, "Flow of top coal and roof rock and loss of top coal in fully mechanized top coal caving mining of extra thick coal seams," *Arabian Journal of Geosciences*, vol. 9, no. 6, pp. 1–9, 2016.

[13] C. Meng and X. H. Li, "Analysis and application of parameters sensitivity of bolt support in gob-side entry driving," *China Coal*, vol. 39, no. 3, pp. 45–49, 2013.

[14] Y. Yuan, S. H. Tu, X. G. Zhang, and B. Li, "Dynamic effect and control of key strata break of immediate roof in fully mechanized mining with large mining height," *Shock & Vibration*, vol. 2015, no. 4, 11 pages, Article ID 657818, 2015.

[15] J. B. Bai, W. L. Shen, G. L. Guo, X. Y. Wang, and Y. Yu, "Roof deformation, failure characteristics, and preventive techniques of gob-side entry driving heading adjacent to the advancing working face," *Rock Mechanics and Rock Engineering*, vol. 48, no. 6, pp. 2447–2458, 2015.

[16] B. X. Li, Y. Li, W. S. Zhu, C. Li, and Z. X. Dong, "Impact of in situ stress distribution characteristics on jointed surrounding rock mass stability of an underground cavern near a hillslope surface," *Shock and Vibration*, vol. 2017, no. 1, 10 pages, Article ID 2490431, 2017.

[17] H. S. Wang, D. S. Zhang, L. Liu et al., "Stabilization of gob-side entry with an artificial side for sustaining mining work," *Sustainability*, vol. 8, no. 7, pp. 1–17, 2016.

[18] J. B. Bai, *Control Mechanism about Gateway Driven along Goaf*, China University of Mining and Technology press, Beijing, China, 2006.

[19] M. G. Qian, X. X. Miao, and F. L. He, "Analysis of key block in the structure of voussoir beam in longwall mining," *Journal of China Coal Society*, vol. 19, no. 6, pp. 557–563, 1994.

[20] H. Q. Shuang, H. S. Wang, S. G. Li, X. Z. Zhang, L. Z. Wu, and Y. J. Dong, "Reasonable width optimization of narrow coal pillar in roadway driven along goaf of fully mechanized caving face," *Coal Engineering*, vol. 47, no. 2, pp. 18–21, 2015.

[21] H. S. Wang, X. Z. Zhang, L. Z. Wu, S. G. Li, and Y. J. Dong, "Surrounding rock control technology of roadway in "isolated island" fully mechanized coal face," *Coal Technology*, vol. 30, no. 8, pp. 83-84, 2011.

[22] H. S. Wang, S. G. Li, X. Z. Zhang, L. Z. Wu, Y. J. Dong, and H. Q. Shuang, "Analysis on stability of narrow coal pillar influenced by main roof fracture structure of gob-side roadway," *Coal Science and Technology*, vol. 42, no. 2, pp. 19–22, 2014.

[23] H. Q. Shuang, *Study on Stability Analysis and Control Technology about Roadway Driving along Goaf at Fully Mechanized Top Coal Caving*, Xi'an University of Science and Technology, Xian, China, 2015.

[24] W. Jiang, W. J. Ju, Z. L. Wang, Z. Zhang, and M. Shi, "Characteristics of overburden stress distribution and rational pillar width determination of gob-side roadway with thick and hard basic roof in fully mechanized top coal caving workface," *Journal of Mining and Safety Engineering*, vol. 37, no. 6, pp. 1142–1151, 2020.

[25] X. J. Meng, "Solid coal rib support technology of fully-mechanized mining along gob-side entry driving based on main roof fracture location," *Coal Science and Technology*, vol. 48, no. 1, pp. 61–68, 2020.